

GUIDA: A Graphical User Interface for Optical Data Analysis of Isolated Pulsars

F. AMBROSINO

Istituto Nazionale di AstroFisica, Osservatorio Astronomico di Roma, Monte Porzio Catone, Via Frascati, 33 00040; La Sapienza-Università di Roma, P.le Aldo Moro, 5, 00185; and Tor Vergata-Università di Roma, Via Orazio Raimondo, 18, 00173,
Italy; filippo.ambrosino@oa-roma.inaf.it, filippo.ambrosino@roma1.infn.it

Received 2015 April 10; accepted 2015 June 27; published 2015 August 27

ABSTRACT. Studying pulsars from ground-based telescopes needs data analysis to be performed according to specific requirements. Because of the periodic behavior of these objects such requirements are expressed in terms of timing. In fact, several factors must be taken into account to correctly extract the period (frequency) and then light curves of pulsars. Until now, analysis software packages have been mainly developed for satellite data and are not completely suitable for optical observations from the ground. A software package called GUIDA has been developed to analyze optical photometric data recorded by the SiFAP instrument, completely conceived and realized at the Physics Department of La Sapienza-Università di Roma. This software package is capable of analyzing data relative to ground observations, including timing corrections, and of deriving corrected pulsar light curves.

Online material: color figures

1. INTRODUCTION

Ground-based observations are often very problematic and complex because of a lot of factors. Among them, the terrestrial atmosphere and the fact that the Earth does not belong to an inertial frame system must surely be considered. In this type of system, a clock does not tick at a constant rate, but is a differential quantity because of the Earth's rotation and revolution around the Sun.

Timing constitutes a fundamental problem that must be taken into account when performing data analysis (especially on pulsars). For this reason, an inertial (or quasi-inertial) frame system must be chosen. Such a system is identified in the SSB (solar system barycenter).

In fact, if the origin of the coordinates is located at the SSB, it is possible to consider it as a fixed stable point and then to compute timing corrections starting from the ephemerides of the SSB, Sun, and Earth.

Several corrective timing factors have to be included to perform a complete analysis of an isolated pulsar. All these quantities will be presented and discussed in the next sections.

If the pulsar belongs to a binary system, further terms must be considered (e.g., center of gravity of the system).

Building a corrected pulsar light curve thus requires a precise estimate of all corrective factors. Unfortunately, until now most of the analysis software packages have been conceived for satellite applications and data.

The GUIDA (graphical user interface for data analysis) software package has been developed and used to analyze data collected by the SiFAP (silicon fast astronomical photometer)

instrument (Meddi et al. 2012; Ambrosino et al. 2013) from ground-based observations.

The SiFAP instrument is a three-channel, fast photometer (conceived and realized at the Physics Department of La Sapienza-Università di Roma), whose properties make it particularly suitable for observations of variable objects (like pulsars) in the optical band.

Each channel is composed of a MPPC (multipixel photon counter) module, manufactured by the Hamamatsu Photonics firm,¹ and custom electronics called P3E (pulsar pulse period extractor).

The three channels are dedicated to different sources: variable object (Channel 0), nearby sky (Channel 1), and reference star (Channel 2). MPPC sensors receive source radiation and convert it into transistor–transistor–logic-compatible pulses by a comparator (discriminated output). These pulses are then counted into time gates from 100 ms down to 1 ms.

A FPGA (field-programmable gate array) internal to the P3E electronic chain integrates them into fixed time windows of 0.02 ms instead.

Studying photometry of variable phenomena requires UTC (universal time coordinated) to be linked to measurements. Such a control is well achieved thanks to an optical marker superimposed on the signal coming from the source. This marker is driven by a precise electrical pulse, called 1PPS (1 pulse per second), generated by a commercial GPS (global positioning

¹ <http://www.hamamatsu.com>.



FIG. 1.—Main panel of GUIDA software package. See text for more details.

system) unit with a time accuracy of $\pm 1 \mu\text{s}$. Further hardware improvements will soon permit it to reach an accuracy of $\pm 25 \text{ ns}$.

The GUIDA package has also been developed to process high time resolution photometric data coming from other ground instrumentations, despite the fact that such a software package has not yet been tested on those data.

The GUIDA package has been realized using a MATLAB environment² and is capable of:

1. applying the whole set of time correction;
2. performing FFT (fast Fourier transform) analysis to extract the spin frequency and thus the spin period of the pulsar;
3. build the pulsar light curve.

2. GUIDA: THE GRAPHICAL INTERFACE

The main panel of GUIDA (shown in Fig. 1) is composed of hidden function blocks, which are interlinked to each other. A block diagram of the interconnection of internal blocks is illustrated in Figure 2.

Some input/output variables used in these function blocks can be often utilized again for further actions, but they cannot

be controlled and modified by the user. The function of the single block will be presented in the following sections.

2.1. Import Data Setting Panel

This panel is dedicated to the settings for importing data. The file to be analyzed must be chosen by the *Browse...* button, as shown in Figure 3. Such a file must contain both time and count vectors. A window will appear and will allow selection of the file. The complete path will be displayed in the *File Location* box. In addition, the panel provides the choice of either ASCII-formatted or binary files.

If the selected file is an ASCII file, the time format must be set by enabling one of the three option buttons:

1. *Index*, if the time vector is a progressive index;
2. *s*, if the time vector is in seconds;
3. *JD*, if the time vector is a Julian Date.

Otherwise, if the file is a binary file, raw data encoding must be previously selected from the listbox labeled *Binary Encoding* by choosing among 8-, 16-, and 32-bit data.

Before importing a file, the *Gate Time* box needs to be filled with the sampling time bin, expressed in seconds. Then, the specified file can be opened by the *Import File* button.

² <http://www.mathworks.com>.

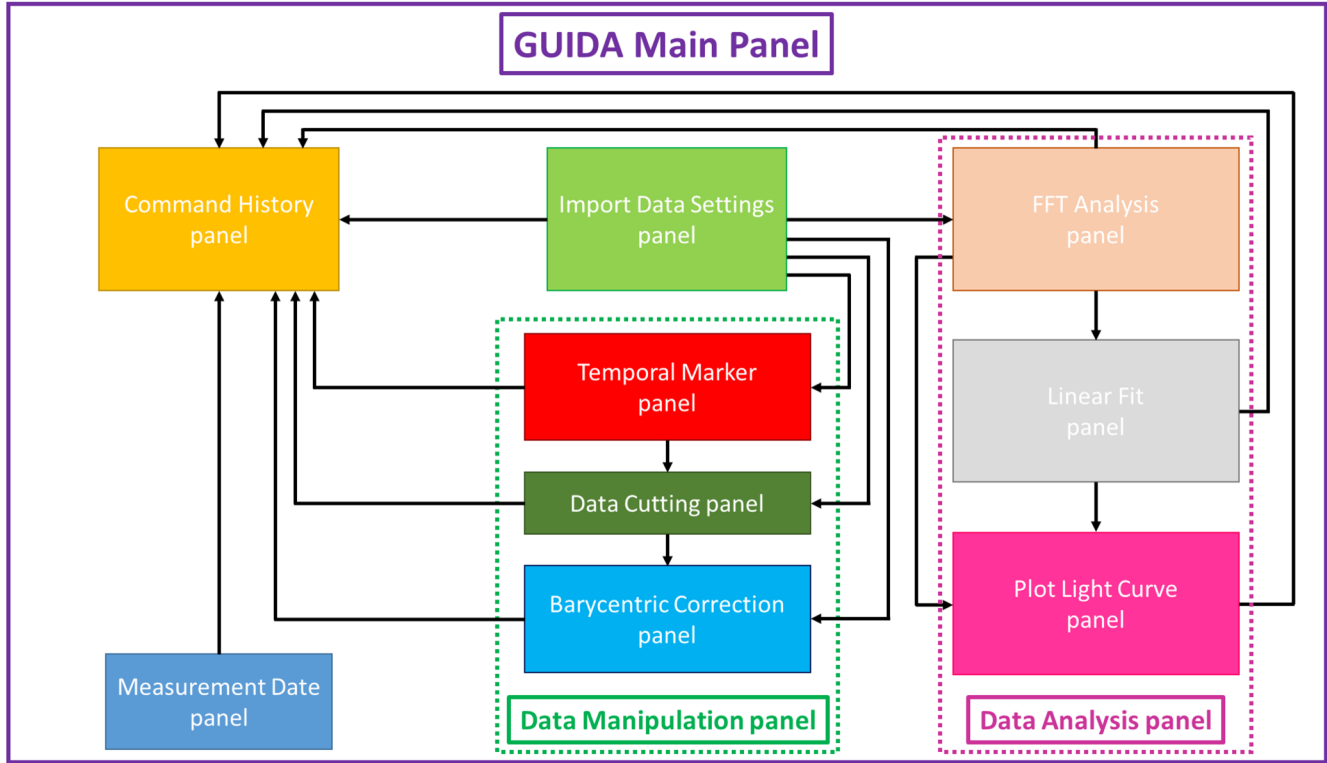


FIG. 2.—Block diagram of the interconnections among function blocks. Some variables cannot be extracted for modification. See the electronic edition of the *PASP* for a color version of this figure.

2.2. Measurement Date Panel

The time unit for astronomical observations is expressed as JD or as MJD (Modified Julian Date) by international convention. The *Measurement Date* panel allows the conversion from UTC date format (hh/mm/ss dd/mm/yyyy) into JD.

The panel is shown in Figure 4; it is particularly useful because it allows a built-in time conversion interface without any additional loss of time in using other softwares.

Blank boxes labeled with day, month, year, hour, minute, and second relative to both start and stop measurement time must be

filled. The *Calculate JD* button allows the computation of both the start and stop acquisition time, expressed as JD. The result of the calculation will appear in the *Command History* window.

2.3. Data Manipulation Panel

The study of pulsars requires establishing a precise reference time, except for measurements done by using JD as the time unit. As usual, a reference time can be generated using a GPS, which provides both coordinate and time information.

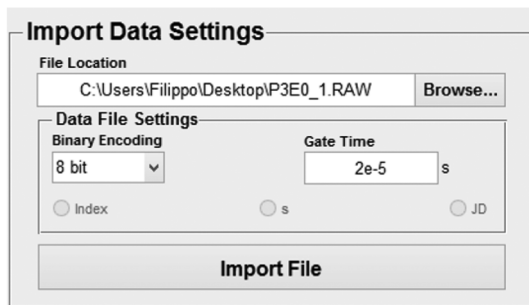


FIG. 3.—Importing data panel. The file to be analyzed can be chosen by browsing through all folders on the PC. It is possible to select either ASCII-formatted or binary files.

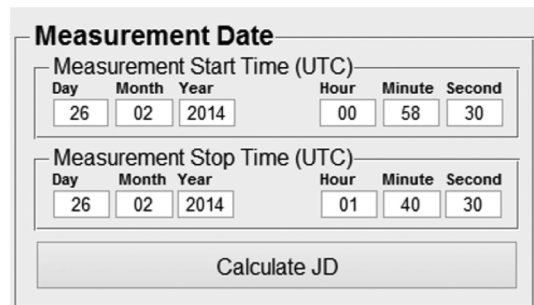


FIG. 4.—*Measurement Date* panel. This panel allows the conversion of acquisition time from UTC format to JD format.

In addition, the GPS can be configured to give an output periodic electrical signal, called 1PPS, linked to the time information.

As in the case of SiFAP, such a signal can be suitably converted and then used as an optical temporal marker superimposed on the data (Meddi et al. 2012; Ambrosino et al. 2013). The rising edges of this pulse-shaped marker are related to the UTC provided by the GPS, giving information about the marker time of arrival. Two pulses are usually used to define both the start and stop time of measurements. The panel is presented in Figure 5.

In order to extract time information from marker rising edges, both a pulse intensity threshold and a time-separation-between-pulses threshold must be set by filling the boxes labeled *Pulse Amplitude Threshold* and *Pulse Time Separation*, respectively.

The *Retrieve Pulse Rising Edges* button selects rising edges of pulses that are brighter than the threshold specified in the *Pulse Amplitude Threshold* box and more distant in time than the quantity specified in the *Pulse Time Separation* box. UTC linked to these pulses will always be displayed in the *Command History* panel. Pulses that do not satisfy these requirements are discarded.

In addition, in the case of two pulses (start and stop ones), there is the possibility of computing an average sampling time bin, which takes into account possible systematic or stochastic variations due to many factors (e.g., system clock instability and temperature).

Such a computation can be performed only if the effective total duration of the measurement (time between the rising edges of the two pulses) is well known. In fact,

$$\langle \Delta t_{\text{bin}} \rangle = \frac{t_m}{N_b}, \quad (1)$$

where $\langle \Delta t_{\text{bin}} \rangle$ is the average sampling time bin, t_m is the total duration of the measurement expressed in seconds, and N_b is

FIG. 5.—*Data Manipulation* panel. “Retrieve pulse rising edges” function allows both time information and calculation of an average sampling time bin corrected for systematic and stochastic effects.

the total number of time bins between the rising edges of the two pulses.

This computed value will be reported in the box labeled *Effective Gate Time* and can be used for the subsequent FFT analysis.

In addition, data can also be cut either to remove pulses or to limit the analysis to a short section of them by selecting a new start and stop time for the acquisition. This action requires the boxes labeled *New Start* and *New Stop* to be filled with values according to the time measurement limits that are displayed, as usual, in the *Command History* panel.

The cutting data function is executed by the *Cut Data* button, while the saving data action is performed by the *Save Data* button.

2.4. Barycentric Correction Panel

In § 1, the problem of timing in the Earth frame system as a noninertial frame system has been discussed preliminarily. To solve such a crucial problem, some factors must be considered. In fact, the correction process can be expressed as

$$t_B = t + \Delta t_{\text{clk}} + \Delta R_{\odot} + \Delta E_{\odot} - \Delta S_{\odot} - \Delta DM, \quad (2)$$

where t_B is the barycentric arrival time, t is the observed time of arrival, Δt_{clk} are the corrections that convert the local clock time to BDT (barycentric dynamical time), ΔR_{\odot} is the geometrical Rømer delay, ΔE_{\odot} is the Einstein delay, ΔS_{\odot} is the Shapiro delay, and ΔDM is the dispersion measure (Lundholm et al. 2011).

The panel reported in Figure 6 is capable of performing such a time correction starting with the pulsar equatorial coordinates right ascension (R.A.) and declination (decl.) at J2000.0 epoch and the choice of the observatory site.

The time correction has been implemented for the geocenter and two sites where SiFAP has been used: Cassini Telescope,

FIG. 6.—*Barycentric Correction* panel. Performing barycentric correction requires pulsar R.A., decl. and observatory site to be specified.

Bologna Astronomical Observatory, Loiano (Italy),³ and Telescopio Nazionale Galileo (TNG), Roque de los Muchachos Observatory, La Palma (Canary Islands, Spain).⁴

These locations have been chosen because they host telescopes (obviously except for the geocenter) from which data have been collected and whose ephemerides have been computed and downloaded by using the Horizons Web interface.⁵

It is necessary to warn that these ephemerides are valid until December 31, 2020, and, after this date, they must be updated. After filling the panel with the parameters explained earlier, the time correction can be performed by using the *Apply Barycentric Correction* button.

2.4.1. Clock Corrections

As stated earlier, the acquisition time vector is generally provided as UTC by a GPS system. Unfortunately, this kind of time does not tick at a constant rate because it belongs to the Earth noninertial frame system and suffers effects due to both the Earth's rotation and revolution around the Sun. The time reference system is thus required to be converted into a constant one through the completion of several steps.

The first step consists in transforming UTC to TAI (international atomic time), where 1 s is defined as the time that a cesium-133 atom at the ground state takes to oscillate exactly 9,192,631,770 times. It is given by

$$\text{TAI} = \text{UTC} + N_{\text{ls}} + 10 \text{ s}, \quad (3)$$

where N_{ls} is the number of leap seconds, applied whenever the difference between UTC and UT1 (Universal Time, also known as astronomical time or solar time, referred to the Earth's rotation) approaches 0.6 s, in order to keep such a difference from exceeding 0.9 s.

Until now (2015 April), the number of leap seconds is 25, but it will be increased to 26 at 23:59:60 UTC on 2015 June 30, even if 10 s more have to be considered in the difference between TAI and UTC for historical reasons of measurements.

The second step requires converting TAI to geocentric TT (terrestrial time), using the following relation:

$$\text{TT} = \text{TAI} + 32.184 \text{ s}, \quad (4)$$

where 32.184 s is an offset arising from historical reasons.

The last step consists in transforming TT into BDT, which is the time we would have if observing from SSB. An approximate transformation from TT to BDT that takes time dilation effects into account is given by 127 coefficients of the following equation:

$$\begin{aligned} \text{BDT} \approx & \text{TT} + \sum_{i=1}^{93} A_i \sin(\omega_{A_i} T + \phi_{A_i}) \\ & + T \sum_{i=1}^{27} B_i \sin(\omega_{B_i} T + \phi_{B_i}) \\ & + T^2 \sum_{i=0}^5 C_i \sin(\omega_{C_i} T + \phi_{C_i}) \\ & + T^3 D \sin(\omega_D T + \phi_D), \end{aligned} \quad (5)$$

where A_i , B_i , C_i , and D are coefficients expressed in μs ; ω_{A_i} , ω_{B_i} , ω_{C_i} , and ω_D are angular velocities expressed in $\text{rad}/10^3 \text{ yr}$; and, ϕ_{A_i} , ϕ_{B_i} , ϕ_{C_i} , and ϕ_D are angular phases expressed in rad. T represents the number of Julian centuries since the start of the J2000.0 epoch and is defined as

$$T = \frac{JD - 2,451,545}{36,525}, \quad (6)$$

where JD is the acquisition time vector (previously converted into TT), expressed in Julian Date (Fairhead & Bretagnon 1990).

Equation (5) provides an accuracy of 100 ns, but it can be improved to 1 ns by implementing all 750 coefficients in the equation instead of 127.

A more detailed explanation about how these coefficients have been computed can be found in Fairhead & Bretagnon (1990).

2.4.2. Geometrical Correction: Rømer Delay

The geometrical correction, shown in Figure 7, is due to the variation of the distance between the observation site and the pulsar while the Earth is turning on itself and moving around the Sun. The Danish astronomer Rømer was the first to study this kind of problem, and the time delay of the light reaching us, due to the effects cited above, is the so-called ‘‘Rømer delay.’’

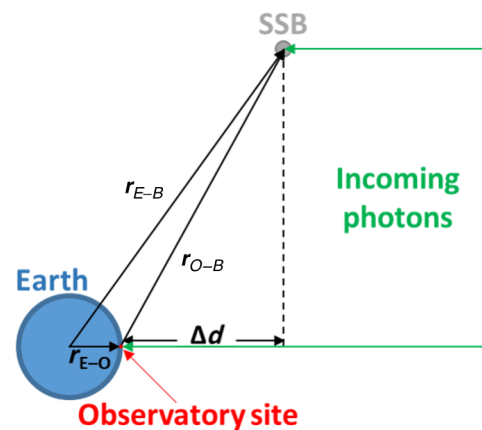


FIG. 7.—Schematic representation of the geometrical system. Vector quantities are explained in the text. See the electronic edition of the *PASP* for a color version of this figure.

³ <http://www.oabo.inaf.it>.

⁴ <http://www.tng.iac.es>.

⁵ <http://ssd.jpl.nasa.gov/horizons.cgi>.

Considering that both the vector \mathbf{r}_{E-B} pointing from geocenter to SSB and the vector \mathbf{r}_{E-O} pointing from geocenter toward the observatory site are known, it is possible to compute the vector \mathbf{r}_{O-B} pointing from the observatory site toward SSB as the difference $\mathbf{r}_{O-B} = \mathbf{r}_{E-B} - \mathbf{r}_{E-O}$ (Lundholm et al. 2011).

The paths of incoming photons from the pulsar (considered to originate at infinity) are, to a good approximation, parallel in the whole solar system. For targets located close to our solar system, further corrections due to parallax can be included in addition to the geometrical correction.

Considering such an approximation, hence, the formula for geometric time correction (i.e., Rømer delay, ΔR_{\odot}) is given by

$$\Delta R_{\odot} = \frac{\mathbf{r}_{O-B} \cdot \hat{\mathbf{n}}}{c}, \quad (7)$$

where $\hat{\mathbf{n}}$ is the unit vector for the incoming photons, and c is the speed of light (Lundholm et al. 2011).

2.4.3. Relativistic Correction: Einstein and Shapiro Delay

The Einstein delay is the combined effect of gravitational redshift and time dilation due to motions of the Earth and other bodies and is caused by the time-varying gravitational potential and Doppler shifts experienced by the observatory clock.

The first effect is corrected by equation (5), considering the clock to tick as it would on SSB, while the second one can be estimated and corrected by using the ephemerides of observatory site.

The analytical relation that represents the Einstein delay (ΔE_{\odot}) is given by

$$\Delta E_{\odot} = \frac{\mathbf{r}_{E-O} \cdot \mathbf{v}_{\text{Earth}}}{c^2}, \quad (8)$$

where $\mathbf{v}_{\text{Earth}}$ is the velocity of the Earth relative to SSB.

The Shapiro delay is caused by space–time curvature around massive objects due to their gravitational field. In fact, when light passes close to a massive object, its trajectory will be curved, so that when it reaches the observer it will not have traveled in a straight line. Because a curved path is longer than a straight line, the light will need more time to reach the observer.

The analytical relation that describes the Shapiro delay (ΔS_{\odot}) is given by

$$\Delta S_{\odot} = -\frac{2GM_{\text{object}}}{c^3} \ln(1 + \cos(\theta)), \quad (9)$$

where θ is the angle between the pulsar and the Earth, as seen from the Sun; G is the gravitational constant, and M_{object} is the mass of the object of which the gravitational field is considered (Lundholm et al. 2011).

2.4.4. Dispersion Measure Delay

The dispersion measure delay term (ΔDM) takes into account the time delay of the propagation of a signal with a certain frequency with respect to one of infinite frequency along a path of length d from the pulsar to the Earth. This time delay is quantified by

$$\Delta DM = \frac{1}{c} \int_0^d \left[1 + \frac{f_p^2}{2f^2} \right] dl - \frac{d}{c} = \mathfrak{D} \times \frac{DM}{f^2}, \quad (10)$$

where f_p is the frequency of partially ionized plasma crossed by a signal of frequency f , e is the fundamental charge, m_e is the electron mass, n_e is the Galactic electron density distribution.

\mathfrak{D} is the dispersion constant, defined as

$$\mathfrak{D} \equiv \frac{e^2}{2\pi m_e c}. \quad (11)$$

DM is the dispersion measure, expressed by

$$DM = \int_0^d \frac{n_e dl}{f^2}. \quad (12)$$

Being proportional to the inverse of the square frequency of the signal, this last quantity can be considered negligible when performing observations in the optical band, but it cannot be neglected in the radio band (Lorimer & Kramer 2005).

2.5. Data Analysis Panel

Once observations have been completed, data analysis will be performed following the steps described below:

1. Perform FFT analysis on either raw or corrected data finding characteristic harmonics (if any) of the pulsar signal;
2. Plot the computed harmonic frequencies as a function of their ordinal number, performing a linear fit to extract the best fundamental harmonic and thus the pulsar spin period;
3. Plot the pulsar light curve by using the period calculated in the previous step.

The procedure described above is shown top to bottom in Figure 8.

2.5.1. FFT Analysis Panel

The top panel illustrated in Figure 8 has the function to perform a FFT analysis on the data. Such an analysis can be performed only if data have been collected at constant sampling temporal gate (frequency), otherwise they must be resampled before.

Characteristic frequencies of the pulsar signal can be retrieved by selecting both peak amplitude and frequency thresholds and then using the *Retrieve Harmonics* button.

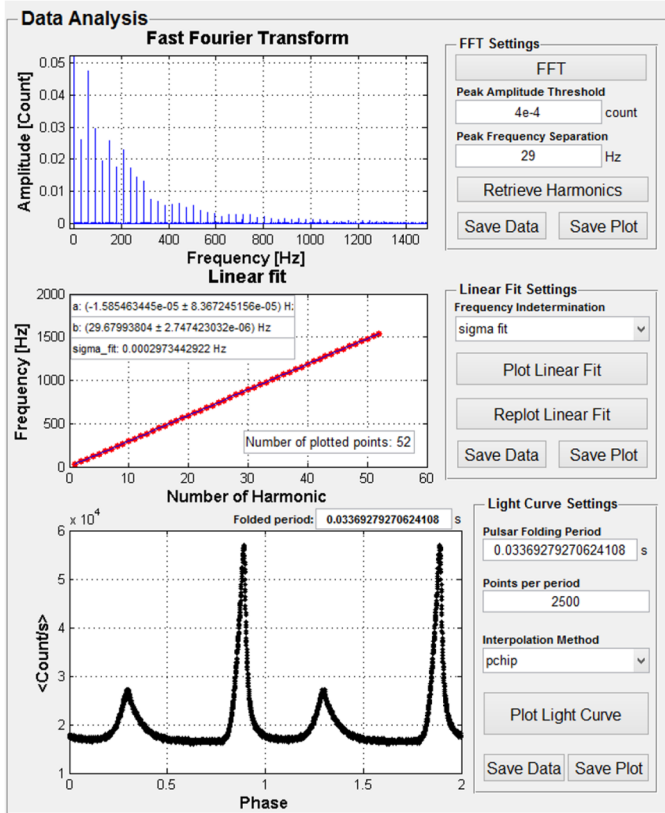


FIG. 8.—*Data Analysis* panel. Three sets of axes with relative setting panels are shown: FFT analysis tool (*top*), linear fitting tool (*center*), and light-curve tool (*bottom*). See the electronic edition of the *PASP* for a color version of this figure.

These two thresholds can be chosen starting from the FFT plot. They only allow selection of frequencies that are well distinguished from noise, in order to have a good linear fit.

In addition, the *Save Plot* and *Save Data* buttons allow storage of both the plot and the analyzed data for any eventual further application.

2.5.2. Linear Fit Analysis Panel

Once the harmonics of the pulsar have been retrieved, it is necessary to find the best spin frequency of the pulsar by performing a linear fit on them.

The middle panel shown in Figure 8 provides such a kind of analysis. Linear fitting is performed once the indetermination on the frequency has been selected between:

1. sigma fit and
2. standard deviation,

where sigma fit implies an indetermination computed by assuming the square root of the sum of the square residuals over the degrees of freedom (DoF) ratio, while the standard deviation is calculated starting from half of the time gate sampling.

Fit parameters will appear in the three boxes at the top left of the panel. Number of plotted points will be shown in the box on the bottom right.

Then, a dialog box will appear asking for the possibility to discard any point from the fit. If so, the linear fit can be iterated and then updated by the *Replot Linear Fit* button.

This procedure can be repeated until the desired linear fit will be displayed with the possibility to save, as a figure, all linear fit plots (and relative terms) generated from the beginning.

As usual, *Save Plot* and *Save Data* buttons allow storage of both the plot and the analyzed data for any eventual further application.

2.5.3 Light Curve Panel

After linear fitting analysis, the pulsar light curve is ready to be folded by using the bottom panel illustrated in Figure 8.

The period calculated by inverting the best value of the harmonic of the pulsar computed by the linear fitting analysis will be displayed in the box labeled *Pulsar Folding Period*, but it can be changed to another value. Before plotting the light curve, it is necessary to select:

- the number of points per period, filling the box labeled *points per period*;
- the interpolation method for building the light curve by choosing among:

1. *nearest*;
2. *linear*;
3. *spline*;
4. *cubic*;
5. *pchip* (similar to cubic).

Once these two parameters have been set, the count per second of the pulsar light curve will be built point by point in the plot as a function of its phase (not related to the Jodrell Bank Observatory ephemerides) by the *Plot Light Curve* button. The folded period will appear in the box located in the top right of the plot.

Once again, *Save Plot* and *Save Data* buttons allow storage of both the plot and the analyzed data for any eventual further applications.

2.6. Command History Panel

During any type of data analysis, it is useful to keep a log document where all actions made are stored. The panel that lists all the actions and commands is shown in Figure 9.

In the blank box, the action/command list given until that moment will appear. The *Save History* button allows saving it into a log file, while the *Clear Display* button allows erasing the listed commands. The *Exit* button allows quitting the main GUI.

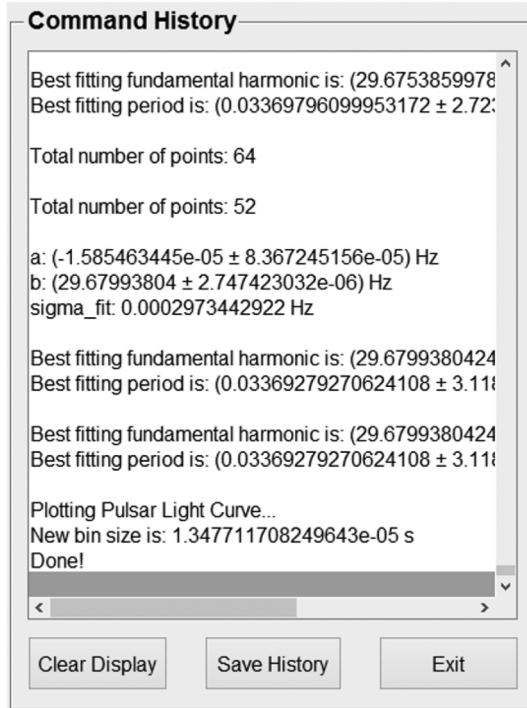


FIG. 9.—*Command History* panel. The contents of the listbox can be stored in a log file. In addition, it is possible to clear the display for a new action/command list and also to quit the main GUI.

3. GUIDA: COMPARISON WITH OTHER SOFTWARES

When a new software is developed, it is mandatory to verify its capabilities. If it is possible, it would also be appropriate to compare it with other preexisting softwares that have already been tested on the same target using both the same instrumentation and data sets.

For this aim, the XRONOS⁶ software package from HEASARC⁷ (High Energy Astrophysics Science Archive Research Center) has been chosen as already existent data analysis software. Data to be analyzed have been selected from those available for the Crab pulsar that have been collected by SiFAP during past observations.

If data are stored in ASCII files, it is mandatory to convert them into FITS ones so they can be read by the XRONOS package.

The procedure used in analyzing the Crab pulsar data using XRONOS software is reported below:

1. Utilize the *earth2sun* tool to perform the barycentric corrections (as discussed in § 2.4), although this tool uses an older version of ephemerides (with respect to the ones utilized in the

GUIDA package), which does not include relativistic corrections and computes corrections at the geocenter only.

2. Use the *efsearch* tool, which is capable of computing the best spin period of the pulsar.

3. Exploit the *efold* tool to plot the pulsar light curve by using the period computed by the *efsearch* tool.

On February 26, 2014, the *SiFAP* instrument observed the Crab pulsar at the TNG, acquiring its signal for about 2500 s.

To compare the results obtained by using both the XRONOS and GUIDA software packages, data analysis has been performed on a smaller portion (1000 s) of the total acquisition because of a critical memory problem in converting ASCII files into FITS ones on the XRONOS side. The processed data have been selected from those collected by the P3E electronic chain relative to the target (Channel 0).

The best spin period computed by the *efsearch* tool (after applying the barycentric corrections) is equal to $(0.033692795 \pm 0.000000023)$ s.

A pulsar light curve has been built by using such a period, and it is shown in Figure 10.

Analyzing the same data with the GUIDA software gives a best-fit spin period for the Crab pulsar equal to $(0.0336927927 \pm 0.0000000031)$ s. This result has been reached by following the procedure described in the § 2.5 (see Fig. 8), correcting data at geocenter.

The comparison between the results of data analysis done by using the two software packages shows an agreement within 5 ns for the computed spin period of the pulsar (which is within the errors).

In addition, the plotted light curves are almost identical. Such a statement is confirmed by considering the values reported on both the *x*- and *y*-axes of the plots (see the bottom panels of Figs. 8 and 10).

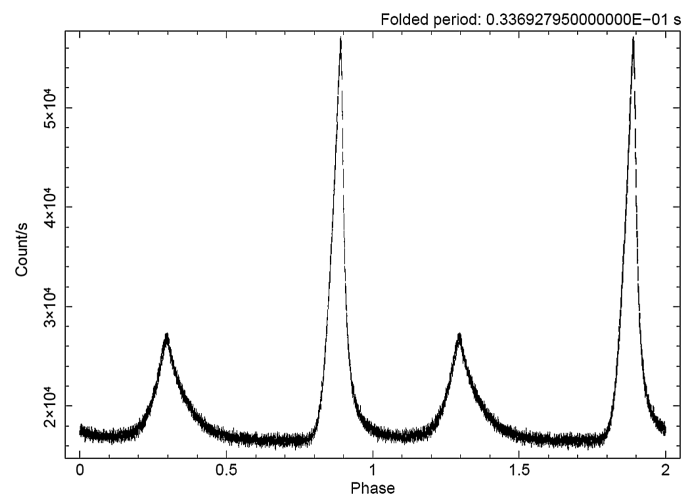


FIG. 10.—Crab pulsar light curve. The folded period has been computed by using the *efold* tool after the barycentric corrections performed by the *efsearch* tool.

⁶ <http://heasarc.gsfc.nasa.gov/xanadu/xronos/xronos.html>.

⁷ <http://heasarc.gsfc.nasa.gov>.

In fact, the possibilities of the GUIDA package are also confirmed by comparing the computed spin period of the Crab pulsar with the one tabulated by the JBO⁸ (Jodrell Bank Observatory of Manchester). JBO tabulates the spin frequency of the Crab pulsar every month; the procedure used to extract the spin period has been the following:

1. Perform a parabolic fit to the tabulated spin frequencies as a function of MJD (Modified Julian Date).
2. Calculate fit parameters with errors.
3. Interpolate (or extrapolate) the frequency value at the desired MJD.
4. Compute both the spin period (from the interpolated frequency) and its relative error.

Applying the procedure mentioned earlier, the computed value for the spin period of the Crab pulsar is equal to $(0.03369294 \pm 0.00000077)$ s. Such a result is widely compatible with the one obtained by performing data analysis with the GUIDA package.

4. CONCLUSIONS

Until the last decade, data analysis was often performed using command-shell-based softwares, but now graphical interface softwares are becoming increasingly popular, simplifying

data analysis a lot and reducing computing time. The GUIDA software package has been developed to reach such a goal.

In fact, very good results can be obtained, considering the performance of similar, preexisting softwares (e.g., XRONOS^{5,6}).

The novelty of the GUIDA package lies in analyzing data while applying all necessary time corrections (both geometrical and relativistic). Data can now be analyzed using a GUI rather than with a command shell (as in older software packages like XRONOS). A graphical interface is more versatile and effective because it provides concrete knowledge of how the data analysis is progressing. In addition, the GUIDA package is capable of manipulating and processing huge amounts of data, avoiding the necessity of splitting them into smaller data sets.

Although the current version of the GUIDA software package can perform robust data analysis, it could be improved by introducing some additional features.

First of all, a new algorithm for the spectral analysis could be implemented, even with nonconstant sampled data.

Further improvements could be both providing the ability to insert the ephemerides of other observatory sites and completing equation (5) by adding missing terms in order to have an accuracy down to 1 ns, compared to the 100 ns actually adopted in the present version of the GUIDA software package (see § 2.4.1).

The last point concerns barycentric corrections, which can be extended to pulsar binary systems by adding corrective terms that also take into account the center of gravity of the system in equation (2).

REFERENCES

- Ambrosino, F., Meddi, F., Nesci, R., Rossi, C., Sclavi, S., & Bruni, I. 2013, *J. Astron. Instrum.*, 2, 1350006
- Fairhead, L., & Bretagnon, P. 1990, *A&A*, 229, 240
- Lorimer, D. R., & Kramer, M. 2005, *Handbook of Pulsar Astronomy* (Cambridge: Cambridge Univ. Press), 85
- Lundholm, M., Mikhalev, V., & Nilsson, P. 2011, Bachelor degree project, Royal Institute of Technology
- Meddi, F., Ambrosino, F., Nesci, R., Rossi, C., Sclavi, S., Bruni, I., Ruggieri, A., & Sestito 2012, *PASP*, 124, 448

⁸ <http://www.jb.man.ac.uk/pulsar/crab/crab2.txt>.